19) lines reported correspond to those of $ZrCl$[2] when given a constant 1.8% displacement of reported distances. The presence of some ZrCl is not an illogical result of the preparative method since $P(ZrCl_4)$ was well short of that estimated above $ZrCl_3$(s) (Experimental Section—Syntheses). The $ZrCl_2$ pattern reported by the same authors[24] is clearly that of monoclinic ZrO_2.[4]

The nonstoichiometry found for the trihalides as well as the weak binding between strands or crystallites in the fibrous macrocrystals suggests a variety of defects must occur in the real crystals. Diffraction lines forbidden by the space group (a point of some dispute for $ZrCl_3$[5]) have never been observed in powder patterns of any tribromide composition across the entire homogeneity range $2.87 \leq Br:Zr \leq 3.23$, even after considerable annealing. But in substoichiometric trichloride a weak and very broad 001 band (6–10 times normal line width) is generally present, especially at the lower limit, although no extra lines have ever been found in Guinier patterns of the slightly superstoichiometric chloride. On the other hand, triiodide samples at the upper limit exhibit three symmetry-forbidden reflections as weak but sharp lines (001, 101, 103) along with four other sharp, faint lines at 9.65, 7.43, 3.78, and 2.50 Å. These presumably originate from some superstructure analogous but not identical with that deduced for the superstoichiometric hafnium triiodide.[18]

There is not much which can be added to the earlier[18] speculation regarding the likely mechanism for superstoichiometry involving normal cation sites, viz., $4Zr^{3+} = 3Zr^{4+} + V_{Zr}$. Extended Zr–Zr interactions and delocalization which presumably (but not assuredly) occur along the metal chains would thus be interrupted. Of course, displacement of zirconium(III) or zirconium(IV) atoms to isolated positions in otherwise empty octahedral chains is possible, even at stoichiometry, thereby severely limiting the possibility of significant one-dimensional conductivity. No substantial electron conduction in these materials along the chains has ever been found. With two metal atoms per cell a splitting of the presumed band to give an insulating material has been proposed.[25] The simplest substoichiometry mechanism would appear to be the interchain substitution of additional metal atoms (i.e., $Zr_{1+x}X_3$), with possible electron transfer to the chains already present, but long-range organization of these additional defects into proposed[13] 001 shear planes is not evident to x rays.

In all compounds studied oxidation (metal elimination) is accompanied by a logical contraction of the *ab* plane over the entire composition range (Figures 1, 2). In $ZrBr_3$ and $ZrCl_3$ oxidation also yields contraction in *c*, suggesting that elimination of metal atoms is more than compensated by increased binding by the high oxidation states left behind or, perhaps better, that the metal–metal bonding holds the halogen layers apart somewhat. But with the largest iodide, the *c*/*a* ratio is the smallest, the observed *c* dimension elongation with oxidation for both ZrI_3 and HfI_3 is exactly opposite, and only here do superlattice effects appear on oxidation. Additional investigations are certainly needed to clarify the nonstoichiometry as well as conduction processes.

Acknowledgment. This work was supported by the U.S. Department of Energy, Division of Basic Energy Sciences.

Registry No. $ZrCl_3$, 10241-03-9; $ZrBr_3$, 24621-18-9; ZrI_3, 13779-87-8.

References and Notes

(1) A. W. Struss and J. D. Corbett, *Inorg. Chem.*, **9**, 1373 (1970).
(2) D. G. Adolphson and J. D. Corbett, *Inorg. Chem.*, **15**, 1820 (1976).
(3) R. L. Daake and J. D. Corbett, *Inorg. Chem.*, **16**, 2029 (1977).
(4) A. Cisar, R. L. Daake, D. H. Guthrie, and J. D. Corbett, to be submitted for publication.
(5) L. F. Dahl, T. Chiang, P. W. Seabaugh, and E. M. Larsen, *Inorg. Chem.*, **3**, 1236 (1964).
(6) J. A. Watts, *Inorg. Chem.*, **5**, 281 (1966).
(7) J. Kleppinger, J. C. Calabrese, and E. M. Larsen, *Inorg. Chem.*, **14**, 3128 (1975).
(8) E. M. Larsen, J. W. Moyer, F. Gil-Arnao, and M. J. Camp, *Inorg. Chem.*, **13**, 574 (1974).
(9) E. M. Larsen and J. J. Leddy, *J. Am. Chem. Soc.*, **78**, 5983 (1956).
(10) S. I. Troyanov, V. I. Tsirel'nikov, and L. N. Komissarova, *Izv. Vyssh. Uchebn. Zaved., Khim. Khim. Tekhnol.*, **12**, 851 (1969).
(11) H. L. Schläfer and H. Skoludek, *Z. Anorg. Allg. Chem.*, **316**, 15 (1962).
(12) H. L. Schläfer and H.-H. Wille, *Z. Anorg. Allg. Chem.*, **327**, 253 (1964).
(13) D. B. Copley and R. A. J. Shelton, *J. Less-Common Met.*, **20**, 359 (1970).
(14) A. S. Normanton and R. A. J. Shelton, *J. Less-Common Met.*, **32**, 111 (1973).
(15) S. I Troyanov and V. I. Tsirel'nikov, *Zh. Fiz. Khim.*, **48**, 1988 (1974).
(16) S. I. Troyanov, G. S. Marek, and V. I. Tsirel'nikov, *Zh. Fiz. Khim.*, **48**, 2671 (1974).
(17) F. R. Sale and R. A. J. Shelton, *J. Less-Common Met.*, **9**, 64 (1965).
(18) A. W. Struss and J. D. Corbett, *Inorg. Chem.*, **8**, 227 (1969).
(19) J. D. Corbett, R. L. Daake, K. R. Poeppelmeier, and D. H. Guthrie, *J. Am. Chem. Soc.*, **100**, 652 (1978).
(20) F. R. Sale and R. A. Shelton, *J. Less-Common Met.*, **9**, 60 (1965).
(21) E. M. Larsen, private communication, 1977.
(22) B. Swaroop and S. N. Flengas, *Can. J. Phys.*, **42**, 1886 (1964).
(23) B. Krebs, *Angew. Chem.*, **81**, 120 (1969).
(24) B. Swaroop and S. N. Flengas, *Can. J. Chem.*, **43**, 2115 (1965).
(25) G. D. Stucky, A. J. Schultz, and J. M. Williams, *Annu. Rev. Mater. Sci.*, **7**, 321 (1977).

Contribution from the Technical University of Denmark, Chemistry Department A, DK-2800 Lyngby, Denmark

Lower Oxidation States of Sulfur. 1. Spectrophotometric Study of the Sulfur–Chlorine System in Molten NaCl–$AlCl_3$ (37:63 mol %) at 150 °C

RASMUS FEHRMANN, NIELS J. BJERRUM,* and FINN W. POULSEN

Received September 20, 1977

Four different cationic sulfur species were produced by anodic oxidation of sulfur in a NaCl–$AlCl_3$ (37:63 mol %) melt at 150 °C. Good evidence was found for the existence of S(IV) and for the existence of S(II). The most likely oxidation states for the two other species were found to be +1 and $+^1/_2$. The spectra of S(IV) and S(II) as well as the spectra of the possible S_2^{2+} and S_4^{2+} species were calculated from the measured spectra.

Introduction

It is well-known that sulfur in analogy with selenium and tellurium is able to form low positive oxidation states in acidic media such as $H_2S_2O_7$, HSO_3F, HF + SbF_5, and SO_2 + SbF_5.[1,2] It is also possible to stabilize some of these oxidation states in crystals with SO_3F^-, AsF_6^-, SbF_6^-, and $Sb_2F_{11}^-$ as anions. The species S_4^{2+}, S_8^{2+}, and S_{16}^{2+} have been isolated in this way.[1,2]

Low oxidation states of the chalcogens can also be formed in acidic chloroaluminate melts.[3] In the case of selenium and

0020-1669/78/1317-1195$01.00/0

tellurium, crystal structures show well-defined cations such as Se_8^{2+} and Te_4^{2+} with chloroaluminate anions.[4,5] In solution (i.e., in chloroaluminate melts) Te_4^{2+}, Te_6^{2+}, and Te_8^{2+} have been identified with a resonable probability[6] and in the case of selenium, Se_4^{2+}, Se_8^{2+}, Se_{12}^{2+}, and Se_{16}^{2+} have been found to be the most likely species formed.[7,8] However, in the case of the similar sulfur system (for example, prepared from S + Cl_2 + $AlCl_3$), no crystals (i.e., containing the low oxidation states of sulfur) have been prepared.[3] By cooling the melt, the sulfur is recovered. However, this does not apply to the higher oxidation states of sulfur, since $SCl_4 \cdot AlCl_3$ (in the form of SCl_3^+,$AlCl_4^-$) and $SCl_2 \cdot AlCl_3$ (probably in the form of SCl^+,$AlCl_4^-$) are well-known as solids.[9,10] It has also been proposed that the compound formed between $AlCl_3$ and S_2Cl_2 is a 2:1 compound ($2S_2Cl_2 \cdot AlCl_3$) instead of a 1:1 compound.[11]

If we now look at the lower oxidation states in molten chloroaluminate melts, the species S_2^{2+}, S_4^{2+}, S_8^{2+}, and S_{16}^{2+} (together with the high oxidation states S(IV) and S(II)) have been proposed to exist.[12] The possibility for the existence of these species have been based partly on performed spectrophotometric and potentiometric measurements and partly on analogy with the similar selenium and tellurium systems.

The present work will concern the higher of these oxidation states (i.e., oxidation states $\geq +^1/_2$).

Experimental Section

$AlCl_3$ was made from the pure metal (99.999%) and HCl gas (made by reaction between concentrated hydrochloric acid and concentrated sulfuric acid) and further purified by sublimation. NaCl (analytical reagent from Riedel-de Haën) was purified by first passing HCl gas (electronic grade from Matheson) over the solid and then through the melt, flushing with pure N_2, and finally filtering the melt. Since none of the sulfur chlorides have a sufficiently low vapor pressure at room temperature to be weighed in a glovebox prior to addition to the melt, the sulfur species were produced electrolytically.

Few high-temperature experiments on molten salt media have been described dealing with spectroscopy of species generated electrolytically in situ. Open-cell arrangements applicable to systems of low vapor pressure in an inert furnace atmosphere have been devised by Bodewig and Plambeck.[13] The possibility of changing the composition of the melt in the optical cell by electrolysis presents advantages over the usual methods involving the use of a large number of cells of varying compositions or those requiring breaking of the seal and resealing to change compositions: Equilibrium is more quickly obtained, samples with any redox ratio are quickly and easily produced, and a given series of measurements can be compared with more reliability.

The cell for the spectrophotometric measurements was made entirely of fused quartz and consisted of a cuvette with an anode of glassy carbon and a cathode of platinum fused into the top (Figure 1). This cell was made so small that it fitted into a standard spectrophotometric furnace.[14] A small outer diameter of the electrode compartment (22 mm) was achieved by placing the sample compartment (E) inside the counterelectrode compartment (D), the two being connected through an internal frit (H).

Vacuumtight seals of the electrode contacts through quartz were made by sealing molybdenum foil (B) (thickness 0.04 mm) electrowelded to 0.7-mm platinum wire (A) into quartz under vacuum. The electrical contact between the platinum wire and the glassy carbon electrode (C) was ensured by fitting the platinum wire into a concentrically drilled hole in the carbon rod. Part of the carbon electrode was fused into a glass tube to avoid direct contact between melt and platinum wire. The glassy carbon rods, 3-mm diameter, type V 10 (Le Carbone-Lorraine), were degassed under vacuum at 1200 °C for 12 h before use.

Suitable porosity of the silica frit (H) was obtained by subsequent depositions of silicic acid in the frit followed by heat treatment at 200 °C.

The solid components of the two-compartment systems were loaded into the cell through 8-mm tubes. These tubes are not shown on Figure 1, since they were sealed off close to the two compartments (see I) before the experiment started. The two tubes were sealed off under the same internal pressure to ensure that melt was not pressed through the frit.

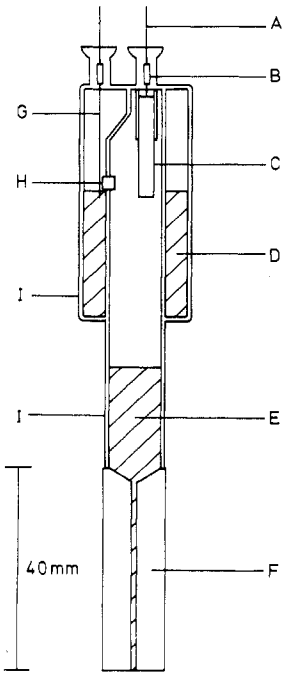

Figure 1. Spectro–electrochemical cell: A, platinum leads; B, vacuumtight molybdenum foil–fused silica seal; C, glassy carbon anode; D, cathode chamber; E, anode chamber; F, optical part of anode chamber; G, platinum cathode; H, silica frit; I, places where loading tubes are sealed off.

During the electrolysis cycle, the cell (and spectrophotometer furnace) was turned upside down, allowing electrolytical contact through the frit. Subsequently it was turned upright and rocked gently until equilibrium was reached (after 1–3 days). The current source for the electrolysis consisted of a calibrated controlled-current, controlled-time device (chronoamperostat) with an accuracy of 0.2%.[15]

The spectra were measured with a Cary 14R spectrophotometer equipped with a Datex digital system for punching out spectral data tape. The furnace used was similar in shape to a furnace described previously,[14] but with independent temperature regulation of the horizontal tube. This furnace was regulated to within ±0.1 °C at 150 °C. The temperature of the furnace was measured by a calibrated chromel–alumel thermocouple to within ±0.5 °C.

General Considerations

The initial molar amount of one of the added substances (in the present work NaCl, $AlCl_3$, sulfur, and chlorine) dissolved in 1 L of the melt is defined as its formality. The density of the NaCl–$AlCl_3$ melt was obtained from the work of Boston[16] (so little sulfur was added to the melt—about 6 mg—that the error introduced by not taking the volume change into consideration was negligible). The ratio between two formalities is called the formality ratio for these substances and is denoted by the letter R. The formal absorptivity is defined by A/lc', where A is the absorbance corrected for the absorbance of cell and solvent, l is the path length, and c' is the formality. Due mainly to the reaction $Al_2Cl_7^- + Cl^- \rightleftharpoons 2AlCl_4^-$, the melt was well buffered with respect to the chloride activity.[17] The obtained spectra were treated with a linear least-squares method developed especially for our spectral work.[6,7,15,18] Similar methods are known from the literature.[19,20] The method used is based on the Bouguer–Beer law and the law of additive absorbances expressed as a general equation involving three matrices, i.e.

$$[l_m c_{mi}][\epsilon_i(\nu'_n)] = [A_m(\nu'_n)] \quad (1)$$

where l_m is the path length at the mth composition, c_{mi} is the concentration of the ith species for the mth composition, $\epsilon_i(\nu'_n)$ is the molar absorptivity of the ith species at the wavenumber

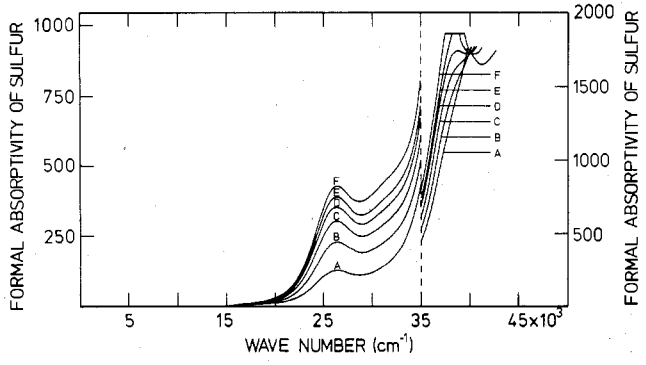

Figure 2. Series of spectra of different sulfur species in NaCl–$AlCl_3$ (37:63 mol %) at 150 °C produced by anodic oxidation of elemental sulfur. Note that two different absorptivity scales have been used. Formality of sulfur was 0.0395_7. S:Cl_2 formality ratio: A, 0.605; B, 0.705; C, 0.807; D, 0.908; E 1.01; F, 1.26.

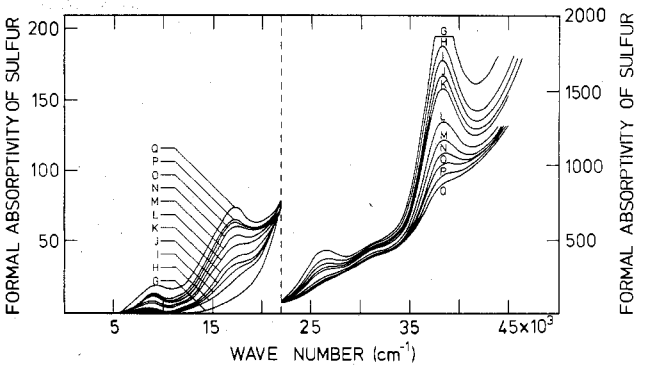

Figure 3. Series of spectra of different sulfur species in NaCl–$AlCl_3$ (37:63 mol %) at 150 °C produced by anodic oxidation of elemental sulfur. Note that two different absorptivity scales have been used. Formality of sulfur was 0.0395_7. S:Cl_2 formality ratio: G, 1.52; H, 2.03; I, 2.28; J, 2.54; K, 2.79; L, 3.57; M, 4.08; N, 4.60; O, 5.12; P, 5.65; Q, 6.17.

ν'_n, and $A_m(\nu'_n)$ is the total absorbance of the mth composition at the wavenumber ν'_n. From one of the models put forward to explain the spectral changes of the melt

$$hS_q^{r+} + jS_y^{z+} \rightleftarrows kS_v^{x+} \quad (2)$$

where h, j, k, q, r, v, x, y, and z are all integers, and from an arbitrarily chosen equilibrium constant, the concentration of each species c_i can be calculated. This (together with the measured absorbances at different wavenumbers and different compositions) can now be introduced in eq 1. Equation 1 cannot be solved exactly (as it is overdetermined in the number of measurements available), but it can be solved in such a way that the best solution (least squares) is obtained, and the deviation between the measured and calculated absorbances can be found. This is most conveniently expressed in the form of variances. The best values of the equilibrium constant in eq 1 (i.e., giving the minimum deviation) are then found by systematic variation. Furthermore, by looking at different models, the minimum variance for each model can be obtained in this way. The ratio between the so obtained minimum variances and the lowest obtained minimum variance (since an independent experimental variance cannot easily be found in this case[15]) is now compared and the probability for each model is now given based on an F test similar to the one used earlier.[6,7] The distinction is made between models with more or less probability than 90% (compared with the model with the lowest variance). Models with higher than 90% probability are marked with an asterisk in the tables.

In all calculations regarding the spectrophotometric work, the variation in the activity coefficients was neglected. This can be justified by the fact that the ionic strength of the solvent was high and the concentration of the solute species was low (less than 0.04 M).

Results and Discussion

Number of Sulfur Species Present in the NaCl–$AlCl_3$ (37:63 mol %) Melt. A whole series of spectra obtained by anodic oxidation of sulfur in NaCl–$AlCl_3$ (37:63 mol %) melt is shown in Figures 2 and 3. The formality of sulfur was 0.0395_7 and the temperature 150 °C. The oxidation was performed with such a low current that no bubbles of chlorine were visible on the anode. It was, therefore, assumed that the sulfur species were probably obtained by direct oxidation and not through formation of chlorine. However, since we are dealing with equilibrium measurements, we will for convenience treat the data as if chlorine was first produced and then reduced by the sulfur. Furthermore, the spectra are for convenience shown in order of increasing reduction (i.e., in the opposite order of the way they were recorded). More measurements than shown in Figures 2 and 3 have been obtained by oxidation of sulfur. These measurements which deal with less oxidized sulfur than given here have been reported elsewhere.[12]

If we now look at Figure 2, it can be seen that the highly oxidized form of sulfur (A) seems to have low absorptivity in the shown range, whereas bands are increasing at 26.4×10^3 and 38.2×10^3 cm^{-1} as the reduction is increased. From Figure 2 it is furthermore clear that the band at 38.2×10^3 cm^{-1} does not follow the band at 26.4×10^3 cm^{-1}. This can most easily be seen by comparing spectra A and B with spectra E and F. The conclusion is, therefore, that we are dealing with at least three sulfur species, one highly oxidized form with maximum concentration for R values (where R is the formality ratio S:Cl_2) below 0.605 (which is the R value for the spectrum A) and two other species at R values in the range from 0.605 to 1.26.

If we now look at Figure 3 (which shows a further development of the spectra when the reduction is increased), it can be seen that the band at 38.2×10^3 cm^{-1} obtains its maximum height (the absorptivity from the other species included) somewhere between spectrum F and spectrum G; a closer analysis shows the same for the band at 26.4×10^3 cm^{-1}. As the reduction is increased, these two bands diminish and two new bands are appearing, one located around 8.7×10^3 cm^{-1} and another at 17.2×10^3 cm^{-1}. A more careful investigation of the spectra reveals that there is a small band located around 31.1×10^3 cm^{-1}. It can be seen that this band first increases and then decreases in such a way that it reaches its maximum size but not its maximum height (i.e., in total absorptivity) somewhere between spectra H and O. Since this increase and decrease is not synchronized with the increase and decrease of the band at 38.2×10^3 cm^{-1} and not with the increase of the two bands at 8.7×10^3 and 17.2×10^3 cm^{-1}, there must be at least two new species present. This is in agreement with the behavior of the band located around 8.7×10^3 cm^{-1}. As the reduction is increased, this band seems to move toward higher wavenumbers (from ca. 8.7×10^3 to ca. 9.3×10^3 cm^{-1}), indicating the presence of at least two species having bands in this wavenumber range. Therefore, altogether, there are at least five sulfur species present in the measured formality ratio range (S:Cl_2) from $R = 0.605$ to $R = 6.17$.

Another way to view the different changes due to the appearance or disappearance of the different species is to plot the absorptivity measured at one wavenumber (in the present case at 26.3×10^3 cm^{-1}) vs. the formality ratio (S:Cl_2). Such a plot is shown in Figure 4. Each data point in this plot is marked with the same letter as the corresponding spectrum. It has been shown that straight lines on such a plot (straight lines which furthermore are independent of the total concentration) are an indication of a two-species system.[6] In the present case, there is no change in the total concentration of

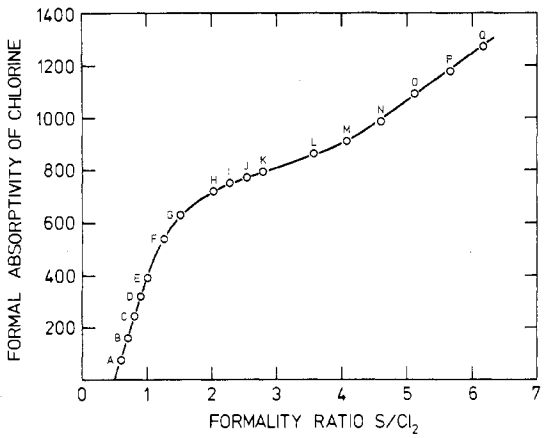

Figure 4. Relation between the formal absorptivity of Cl_2 measured at 26.3×10^3 cm^{-1} and the S:Cl_2 formality ratio. The letters A to Q refer to the spectra marked with the same letters.

sulfur. Therefore the variation in the total concentration cannot be used as a tool to distinguish between real straight lines and lines that look almost straight.[6] A reasonable idea can, however, still be obtained from such a plot. According to the plot in Figure 4, there seem to be only two two-species ranges present in the shown R range. One of these ranges can be found between point A and point D and another range seems to be present between points N and Q. From Figure 4 it can furthermore be seen that there are two (not very well-defined) "breaks" present on the shown plot indicating maximum concentrations of at least one species at each of these "breaks". It can also be seen that the curve as it is drawn does not go through the origin. This must also be due to a "break".

If we look at the positions of these "breaks", it is clear that the first break seems to be located around an R value of 0.5. Unfortunately, no measurements were performed with an R value below 0.5. The next break is located somewhere between $R = 1.0$ and $R = 2.0$. This break is not especially well-defined and there could be two breaks in this range. The next break again is better defined and seems to be located between L and M and close to an R value of 4.0. The plot stops at an R value of 6.17 (spectrum Q). However, some spectra with R values above 6.17 have been published in another connection. According to these measurements, a rather sharp break is found close to an R value of 8.0.[12]

On the basis of Figure 4 and in combination with the knowledge of a break around an R value of 8.0, at least four species must be present in the melt. The most likely oxidation states for these species (based on the R value) are +4, +2 to +1, $+^1/_2$, and $+^1/_4$. However, the conclusion of the discussion about the band positions and variation of band sizes in the spectra was that at least five species were present, so there seems to be one species unaccounted for. Fortunately, we can make comparison with some earlier and preliminary results obtained at 300 °C. These measurements were performed not by anodic oxidation of sulfur but by direct reaction between sulfur and chlorine. The initial amounts of chlorine added to the melt were measured spectrophotometrically in the gaseous state (at the chlorine band located at 30.6×10^3 cm^{-1}). The formal absorptivity of chlorine (measured at 38.1×10^3 and 26.7×10^3 cm^{-1}) vs. R revealed breaks at ca. $^1/_2$, ca. 1, and ca. 8, but there were no indications of breaks at R = ca. 2 and R = ca. 4. The best way to explain this is to assume that species exist corresponding to breaks at $R = {}^1/_2$, 1, 2, 4, and 8 and that at low temperature (i.e., this work) one can obtain all of these species but is not able to distinguish between the two species giving rise to breaks at 1 and 2 (i.e., only one break between 1 and 2 is observed). However, at high temperature (i.e., 300 °C), the species giving rise to the breaks at 2 and 4 disappear making the break at 1 more easily recognized. This explanation makes the existence of five species very likely. The five species will for convenience be labeled from I to V. The most likely formulas for these species (based on the present measurements, i.e., R values) in analogy with what is known about tellurium and selenium[3,6-8] are S(IV), S(II), S_2^{2+}, S_4^{2+}, and S_8^{2+}, where S_8^{2+} obtains its maximum concentration outside the present range of measurements.

Table I. Spectrophotometric Measurements: Variances Obtained for Models[a] with Oxidation States in the Range +6 to +3[b]

Oxidn state	Formal charge 3+	4+	5+	6+
+6				(1.19×10^{-2})
+5			(4.97×10^{-3})	
+4		4.03×10^{-5} *		
+3[c]				

[a] Other species in the equilibria assumed to be S^{2+} and S_2^{2+}. [b] Number of spectra 6; number of different wavenumbers 364; wavenumber range 15.4×10^3 to 35.1×10^3 cm^{-1}; formality ratio (S:Cl_2) range 0.60_5 to 1.26_3; asterisks based on $F_{0.10}(3.3) = 5.39$, indicating models with higher probability than 90%. Parentheses indicate that no minima were found; the values are then for equilibrium constants of either 10^{+60} or 10^{-60}. [c] Variance cannot be calculated.

Formulas for Sulfur Species Present in the NaCl–$AlCl_3$ (37:63 mol %) Melt. We will start with the species with the highest oxidation state. It is clear that the break close to $R = 0.5$ is rather sharp. If we assume that points A to D are lying on a straight line, the cutoff at the abscissa axis can be calculated to be 0.508 ± 0.005. This is very close to $^1/_2$ and since the species with the highest oxidation state has no absorptivity (see later) at the measured wavenumber, this indicates that the oxidation state is +4 for this species. The other breaks are not nearly as sharp as the first break, and, therefore, this method cannot be used to determine the oxidation state of these species.

Another way to treat these data is, as described under the General Considerations, to start with the three-species equilibrium given by eq 2 and the matrix equation given by eq 1. In order to do this, it is important to avoid any four-species ranges. From what has been said above, it is reasonable to assume that we are dealing with mainly two species (I and II) from A to C, three species (I, II, and III) from D to F, possibly four species (I, II, III, IV) from G to H, again possibly three species (III, IV, and V) from I to M, and finally two species (IV and V) from N to Q.

If we now look at the range defined by the spectra A to F where three species should be present and assume that it is most likely that II and III are S^{2+} and S_2^{2+}, respectively, the data given in Table I can be calculated. In this table we have assumed that the oxidation state (and the formal charge) is in the range +3 to +6. From this table it can, as expected, be seen that S^{4+} is by far the best choice for the species with the highest oxidation state.

Another way to treat the data in this range is to assume that the species S^{4+} and S_2^{2+} are known and then try different possibilities for the third species such as S_2^{3+} and S_3^{4+}. The calculations are given in Table II. From this table it can be seen that within 90% probability (see General Considerations) there are only two possibilities both indicating divalent sulfur, namely, S^{2+} or S_2^{4+}. By comparison with similar selenium and tellurium species and from what is generally known about divalent sulfur,[21] S^{2+} is the obvious choice. If we now look at the range from I to Q (R = 2.28 to 6.17) and assume that two of the species in this range are S_4^{2+} and S_8^{2+}, we get the results as shown in Table III. From this table it is obvious that there are many more possibilities than S_2^{2+} for the third species. Even if it has no statistical importance, it should be

Table II. Spectrophotometric Measurements: Variances Obtained for Models[a] with Oxidation States in the Range +4 to +1[b]

Oxidn state	Formal charge 1+	2+	3+	4+
+4[c]				
+3			(3.06×10^{-4})	
+2		0.403×10^{-4} *		0.404×10^{-4} *
$+^3/_2$			3.63×10^{-4}	
$+^4/_3$				3.31×10^{-4}
+1[c]				

[a] Other species in the equilibria assumed to be S^{4+} and S_2^{2+}. [b] Number of spectra 6; number of different wavenumbers 364; wavenumber range 15.4×10^3 to 35.1×10^3 cm^{-1}; $S:Cl_2$ formality ratio range 0.60_5 to 1.26_3; asterisks based on $F_{0,10}(3.3) = 5.39$, indicating models with higher probability than 90%. Parentheses indicate that no minima were found; the values given are then for equilibrium constants of either 10^{+60} or 10^{-60}. [c] Variances cannot be calculated.

Table III. Spectrophotometric Measurements: Variances Obtained for Models[a] with Oxidation States in the Range +2 to +1[b]

Oxidn state	Formal charge 1+	2+	3+	4+
+2		6.46×10^{-5} *		8.62×10^{-5} *
$+^3/_2$			5.50×10^{-5} *	
$+^4/_3$				5.42×10^{-5} *
+1	4.36×10^{-5} *	4.22×10^{-5} *	4.32×10^{-5} *	4.49×10^{-5} *

[a] Other species in the equilibria assumed to be S_4^{2+} and S_8^{2+}. [b] Number of spectra 9; number of different wavenumbers 400; wavenumber range 4.8×10^3 to 43.5×10^3 cm^{-1}; formality ratio ($S:Cl_2$) range 2.28_3 to 6.17_1; asterisks based on $F_{0,10}(6.6) = 3.05$, indicating models with higher probability than 90%.

Table IV. Spectrophotometric Measurements: Variances Obtained for Models[a] with Oxidation States Close to $+^1/_2$[b]

Oxidn state	Formal charge 1+	2+	3+	4+
$+^2/_3$		(5.21×10^{-5})*		(5.21×10^{-5})*
$+^3/_5$			4.46×10^{-5} *	
$+^4/_7$				4.40×10^{-5} *
$+^1/_2$	4.15×10^{-5} *	4.22×10^{-5} *	4.27×10^{-5} *	4.30×10^{-5} *
$+^4/_9$				4.52×10^{-5} *
$+^3/_7$			4.64×10^{-5} *	
$+^2/_5$		4.89×10^{-5} *		5.04×10^{-5} *

[a] Other species in the equilibria assumed to be S_2^{2+} and S_8^{2+}. [b] Number of spectra 9; number of different wavenumbers 400; wavenumber range 4.8×10^3 to 43.5×10^3 cm^{-1}; formality ratio ($S:Cl_2$) range 2.28_3 to 6.17_1; asterisks based on $F_{0,10}(6.6) = 3.05$, indicating models with higher probability than 90%. Parentheses indicate that no minima were found; the values are then for equilibrium constants of either 10^{+60} or 10^{-60}.

noticed that the lowest variance is obtained for S_2^{2+}. However, the conclusion is that the data are not good enough to distinguish between the different models. If we now assume that the other species are indeed S_2^{2+} and S_8^{2+}, calculations as summarized in Table IV can be made. From this table it can be seen that S_4^{2+} has the next lowest variance in this table. However, as before, this has no statistical significance, and the conclusion is here, as before, that more accurate spectrophotometric measurements are needed in order to distinguish between the different models. At present there seems to be no commercial spectrophotometer available for such an improvement.

The spectra of S(IV) and S(II) are given in Figure 5 together with the spectra of the most likely models for the two other species (i.e., S_2^{2+} and S_4^{2+}). From this figure it can be seen that S(IV) has no band maxima and almost no absorptivity in the measured range, whereas S(II) has one band

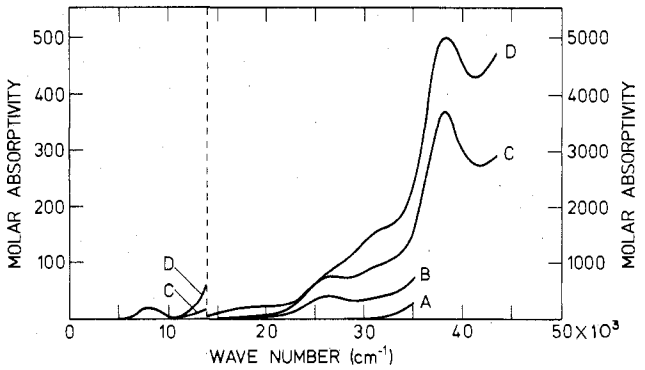

Figure 5. Calculated spectra of the models S^{4+} (A), S^{2+} (B), S_2^{2+} (C), and S_4^{2+} (D).

maximum located at 26.3×10^3 cm^{-1}. If S_2^{2+} is present, it has band maxima at ca. 26.6×10^3 and ca. 38.2×10^3 cm^{-1}. Finally, S_4^{2+} (if it exists) has band maxima at ca. 8.1×10^3 and ca. 38.3×10^3 cm^{-1} and shoulders at ca. 17.6×10^3, ca. 26.5×10^3, and ca. 31.3×10^3 cm^{-1}. The small deviations between these band positions and the band positions given in the section concerning the number of sulfur species present in the melt are due to difficulties in getting the right band positions, when one is dealing with mixtures of different species.

If one compares the spectrum calculated on the basis of a possible S_4^{2+} species with the spectra of the analogous Se_4^{2+} and Te_4^{2+} species in chloroaluminate melts,[6,7] it is clear that there is little resemblance between the present spectrum and the other spectra. The same is the case if we compare the present spectrum with the spectrum of S_4^{2+} in HSO_3F.[22] This spectrum is characterized by a well-defined band at ca. 30.3×10^3 cm^{-1} and a shoulder at ca. 35.7×10^3 cm^{-1}. The first of these bands could in the present case be the band found at ca. 26.5×10^3 cm^{-1}. This is based on the observation for Se_4^{2+} and Te_4^{2+} that the main peaks found in the chloroaluminate melts are located at lower wavenumbers than the main peak found in HSO_3F. To say anything about the next band is difficult. If one compares with Se_4^{2+} and Te_4^{2+} in chloroaluminate melts and in HSO_3F, there is no special tendency for the behavior of this band. Furthermore, it should be noted that a Gaussian analysis of the spectrum of Te_4^{2+} in NaCl–$AlCl_3$[14] gave as the most likely results that the shoulder in this case consisted of two bands. Such an analysis has not been performed on the spectrum of Se_4^{2+} in chloroaluminate melts but it is not unlikely that the best resolution also in this case will give two bands. The band found at ca. 31.3×10^3 cm^{-1} in the present case (or both the band at ca. 31.3×10^3 cm^{-1} and the band at ca. 38.2×10^3 cm^{-1}) could, therefore, be of the same origin as the shoulder (at ca. 35.7×10^3 cm^{-1}) found for S_4^{2+} in HSO_3F. The general shape of the spectrum in Figure 5 is, however, such that it is not very likely that we are dealing with S_4^{2+} (at least not in the square-planar form known for Se_4^{2+} and Te_4^{2+}[5,23]).

In connection with obtaining the spectra of the four sulfur species, the equilibrium constants for the equilibria between the same species are obtained. Since the formulas for two of the species are uncertain, these equilibrium constants are not given in this paper.

Acknowledgment. The authors thank H. A. Andreasen for valuable discussions and L. E. Mikkelsen for designing the spectro–electrochemical cell to our requirements. Further thanks are due to Statens tekniskvidenskabelige Forskningsråd for financial support of R.F. and for computing time at NEUCC (Northern Europe University Computing Center).

Registry No. S(IV), 20681-10-1; S(II), 14127-58-3; S_2^{2+}, 65605-15-4; S_4^{2+}, 12597-09-0; S_8^{2+}, 11062-34-3.

References and Notes

(1) R. J. Gillespie and J. Passmore, *Acc. Chem. Res.*, **4**, 413 (1971).
(2) R. J. Gillespie and J. Passmore, *Chem. Br.*, **8**, 475 (1972).
(3) J. D. Corbett, *Prog. Inorg. Chem.*, **21**, 129 (1976).
(4) R. K. McMullan, D. J. Prince, and J. D. Corbett, *Inorg. Chem.*, **10**, 1749 (1971).
(5) T. W. Couch, D. A. Lokken, and J. D. Corbett, *Inorg. Chem.*, **11**, 357 (1972).
(6) R. Fehrmann, N. J. Bjerrum, and H. A. Andreasen, *Inorg. Chem.*, **15**, 2187 (1976).
(7) R. Fehrmann, N. J. Bjerrum, and H. A. Andreasen, *Inorg. Chem.*, **14**, 2259 (1975).
(8) R. Fehrmann and N. J. Bjerrum, *Inorg. Chem.*, **16**, 2089 (1977).
(9) H. E. Doorenbos, J. C. Evans, and R. O. Kagel, *J. Phys. Chem.*, **74**, 3385 (1970).
(10) S. N. Nabi and M. A. Khaleque, *J. Chem. Soc.*, 3626 (1965).
(11) O. Ruff and H. Golla, *Z. Anorg. Allg. Chem.*, **138**, 17 (1924).
(12) N. J. Bjerrum, "Characterization of Solutes in Non-Aqueous Solvent", G. Mamantov, Ed., Plenum Press, New York, N.Y. 1978, pp 251–271.
(13) F. G. Bodewig and J. A. Plambeck, *J. Electrochem. Soc.*, **117**, 904 (1970).
(14) N. J. Bjerrum, *Inorg. Chem.*, **9**, 1965 (1970).
(15) H. A. Andreasen and N. J. Bjerrum, *Inorg. Chem.*, **14**, 1807 (1975).
(16) C. R. Boston, *J. Chem. Eng. Data*, **11**, 262 (1966).
(17) L. G. Boxall, H. L. Jones, and R. A. Osteryoung, *J. Electrochem. Soc.*, **120**, 223 (1973).
(18) J. H. von Barner, N. J. Bjerrum, and K. Kiens, *Inorg. Chem.*, **13**, 1708 (1974).
(19) Å. Björck, *BIT*, 7, 1,257 (1967).
(20) L. R. Lieto, Thesis, 1969, Report ORNL-TM-2714, Oak Ridge National Laboratory, Oak Ridge, Tenn., 1969.
(21) H. L. Roberts, *Inorg. Sulphur Chem.*, 419–458 (1968).
(22) R. J. Gillespie, J. Passmore, P. K. Ummat, and O. C. Vaidya, *Inorg. Chem.*, **10**, 1327 (1971).
(23) I. D. Brown, D. B. Crump, and R. J. Gillespie, *Inorg. Chem.*, **10**, 2319 (1971).

Contribution from the Paul M. Gross Chemical Laboratory, Duke University, Durham, North Carolina 27706

Electronic Structure of the Tris(ethylenediamine)manganese(II) Ion. Circular and Linear Dichroism and Electron Paramagnetic Resonance Spectra of $Mn(en)_3(NO_3)_2$

RICHARD ALAN PALMER,* MARK CHIN-LAN YANG, and JUDITH C. HEMPEL

Received September 27, 1977

The electronic structure of the tris(ethylenediamine)manganese(II) ion has been investigated by measurement of the orthoaxial linear dichroism (LD), axial absorption, axial circular dichroism (CD), and electron paramagnetic resonance (EPR) spectra of manganese-doped $Zn(en)_3(NO_3)_2$ single crystals. Cotton effects associated with the spin-forbidden ligand field transitions to states derived from $^4T_{2g}(G)$ ($(^4E_g, A_{1g})(G)$) and $^4T_{2g}(D)$ are observed in the CD spectra at 1.98, 2.36, and 2.65 μm^{-1}, respectively, all with the same sign of $\Delta\epsilon$ in a given crystal. These transitions, as well as the lower quartet level $^4T_{1g}(G)$ (1.50 μm^{-1}), not observed in the CD spectra, are also observed in the LD and axial absorption spectra. The sharp band assigned to the $(^4E_g, ^4A_{2g})(G)$ transitions reveals four distinct components at 2.357 ± 0.005, 2.370 ± 0.001, 2.385 ± 0.0005, and 2.395 ± 0.001 μm^{-1} in the absorption spectra. Only the first two of these are prominent in the CD spectra and they are assigned to the origins of the $^4E_g(G)$ and $^4A_{1g}(G)$ transitions, respectively. The ligand field parameters deduced are Dq = 0.108, B = 0.0860, and C = 0.301 μm^{-1}. The EPR data yield $g_\parallel$ = 2.004 ± 0.005 and $g_\perp$ = 2.021 ± 0.005 and A = 77 ± 1, D = +197 ± 10, and $(a - F)$ = (+15 ± 10) × 10^{-4} cm^{-1}. The magnitude and sign of D correlate with the magnitude of the trigonal splitting deduced from the electronic spectrum and the trigonally compressed geometry revealed in the crystal structure of the nickel analogue.

Introduction

As previously reported, the crystals of $Zn(en)_3(NO_3)_2$ are enantiomorphous and are isomorphous with the crystals of the analogous nickel compound.[1,2] The enantiomorphous hexagonal crystal with its D_3 metal site symmetry[3] provides an ideal host lattice for study of the electronic spectra of tris(ethylenediamine) complexes of divalent transition-metal ions, including not only the linear dichroism (LD) but also the circular dichroism (CD). Although the pure crystals of the complexes of nickel(II) and cobalt(II) can be grown, other nitrate salts of tris(ethylenediamine)metal(II) ions are best obtained by cocrystallization with the zinc complex. These include the complexes of copper(II), ruthenium(II), and manganese(II). Of these, the manganese(II) complex is particularly interesting, since relatively few tris(bidentate ligand) chelates of manganese(II) are known. The only previous study of the electronic spectra of such a complex is that of the single-crystal absorption and emission spectra of $Mn(OMPA)_3(ClO_4)_2$.[4] Furthermore, natural optical activity of a manganese(II) complex has previously been reported only for manganese-doped α-$Zn(H_2O)_6SeO_4$.[5] Here we report the single-crystal electronic spectra of $Zn(Mn)(en)_3(NO_3)_2$ (orthoaxial LD, axial CD, and axial absorption) along with correlative data on the electron paramagnetic resonance.

Experimental Section

Crystals of $Zn(en)_3(NO_3)_2$ doped to as much as 10 mol % with manganese(II) were obtained from a N_2-purged, saturated aqueous solution of the zinc compound innoculated with a few drops of concentrated manganese nitrate solution. A small excess of ethylenediamine was present. Crystal growth was by slow evaporation in a glovebag under N_2. The percent manganese in the crystals was determined by atomic absorption. The crystals were cut and polished as previously described.[2]

Absorption spectra and CD spectra were measured using a Cary 14R spectrophotometer and JASCO ORD/CD-5 (SS-20 modification) instrument, respectively. The detailed description of the instrumentation and techniques of recording and treating the data have been given earlier.[1,2] Spectral bandwidth for the Cary 14R was 0.83 Å (slit width 0.025 mm), whereas the minimum for the JASCO instrument was 2.8 A (slit width 0.020 mm). The slit width on the JASCO instrument in the region of the sharp 2.36-μm^{-1} band was adjusted manually to the above value in order to resolve the fine structure more completely. Maximum time constant (64 s) and minimum scan speed were necessary in order to achieve a CD S/N of ≥10 using this reduced slit width. Both the Cary and JASCO instruments were wavelength calibrated using the 4460- and 3608-Å lines of a Ho_2O_3 filter. EPR spectra were measured on a Varian V-4502-15 X-band spectrometer system equipped with frequency- and power-monitoring devices. The concentration of manganese in the crystals used for EPR spectra was ≤1 mol %.

Results

Room-temperature axial absorption and CD spectra are shown in Figure 1. The CD spectrum of the enantiomer with negative Cotton effects for the ligand field bands is chosen for illustration. The assignments of the bands in terms of their octahedral parentages and spectral results in terms of dipole

0020-1669/78/1317-1200$01.00/0